

## Free delta propagator

H. T. Williams

*Department of Physics, Washington and Lee University, Lexington, Virginia 24450*

(Received 1 September 1983)

The free propagator for the spin  $\frac{3}{2}$ , isospin  $\frac{3}{2}$  (delta) particle is discussed, comparing the Rarita-Schwinger formalism and another of Hayward. Its use in the calculation of resonant graphs in pion-nucleon scattering, photon-nucleon scattering, and pion photoproduction from nucleons is exemplified using explicit formulae and numerical results. Predictions using the two formalisms are shown to be in significant disagreement.

### INTRODUCTION

A theoretical description of fields corresponding to particles of nonvanishing mass with spins greater than one-half leads to numerous difficulties: nonuniqueness of the fields, particularly when interactions are considered, has been a problem of some theories; complexity seems inevitable; and gauge freedom produces another level of possible confusion.

For fermions, whereas the spin  $\frac{1}{2}$  seems well described via the Dirac equation, the next most complicated case, spin  $\frac{3}{2}$ , still contains ambiguities. Nuclear physics of the 1980's, as well as theory-based prediction of single nucleon scattering and reaction, seem to require consideration of the delta resonance: spin  $\frac{3}{2}$ , isospin  $\frac{3}{2}$  baryon resonance of mass 1232 MeV and decay width 110 MeV. The broad width of this state precludes its direct detection—it is known by its decay products, or by more subtle effects upon cross sections and decay rates. The calculation of these processes then requires the appropriate propagator for the delta resonance, but not the individual free fields. The purpose of this paper is to examine, compare, and contrast the properties of the free delta propagator from two different theories.

### RARITA-SCHWINGER FORMALISM

At present, the most frequent choice for the relativistic spin  $\frac{3}{2}$  propagator would seem to be that which results from the Rarita-Schwinger<sup>1</sup> equations:

$$\begin{aligned} (\gamma_\mu \partial_\mu + M)\Psi_\alpha &= 0, \\ \gamma_\alpha \Psi_\alpha &= 0, \end{aligned} \tag{1}$$

where the  $\Psi_\alpha$  ( $\alpha=0,1,2,3$ ) are four separate four-component Dirac spinors, the  $\gamma_\mu$  are the standard  $4 \times 4$  matrices of the Dirac theory,  $M$  is the mass of the spin  $\frac{3}{2}$  particle, and repeated indices are assumed summed. The second of the above equations represents supplementary conditions needed to eliminate the redundant spin  $\frac{1}{2}$  solutions possible in the first equation. The propagator in this theory is not without ambiguity. The following form,

$$\frac{2M}{p^2 - M^2 + i\epsilon} \Delta_{\mu\nu} \tag{2}$$

(where  $\Delta_{\mu\nu}$  is the energy projection operator,  $\epsilon$  is a positive infinitesimal, and  $p^2 = E^2 - \vec{p}^2$  is the square of the delta four-momentum), is appropriate for situations where the delta can be considered as comprising a one body intermediate state. The form of the projection operator is

$$\begin{aligned} \Delta_{\mu\nu} = \frac{p_\alpha \gamma^\alpha + M}{2M} \left[ g_{\mu\nu} - \frac{1}{3} \gamma_\mu \gamma_\nu - \frac{2p_\mu p_\nu}{3M^2} \right. \\ \left. + \frac{p_\mu \gamma_\nu - p_\nu \gamma_\mu}{3M} \right], \end{aligned} \tag{3}$$

where  $g_{\mu\nu}$  is the metric tensor.<sup>2</sup> The conventions are those of Bjorken and Drell,<sup>3</sup> and when a specific representation of the  $\gamma$  matrices is needed, that of Appendix A of Bjorken and Drell will be utilized.

The form of the Rarita-Schwinger equations and the propagator derived therefrom is compelling in its similarity to the Dirac spin  $\frac{1}{2}$  results. The Rarita-Schwinger state vector  $\Psi_\mu$  can be seen to consist of, in the nonrelativistic limit, a four-component Dirac spinor and a four-vector coupled in such a way as to produce a total angular momentum of  $\frac{3}{2}$ . The first of the Rarita-Schwinger (RS) equations is simply the Dirac equation on the spinor indices. Nevertheless, the fact that solutions to these equations violate causality has been shown in detail by Velo and Zwanziger.<sup>4</sup> The equations of the RS theory are all covariant, the free propagator shown above is causal, and for that reason perturbation calculations using the theory are causal to all orders. An exact calculation in a situation where there is a quantized external field turns out to be noncausal and Lorentz frame dependent, even in the limit of weak external fields. Velo and Zwanziger show that the problem exists already in the free field equations, manifested by a class of solutions which propagate at speeds exceeding that of light.

### HAYWARD FORMALISM

Presented in contrast to the spin  $\frac{3}{2}$  formalism of Rarita and Schwinger is that from the work of Hayward.<sup>5</sup> This work reports to "... develop a relativistic theory of higher spin fields employing the variational methods of classical Lagrangian field theory. The chief aim is to present an unambiguous method for constructing a dynamical description of a field having any discrete spin. ..." Hayward is successful in that he presents a for-

malism similar for all spins, without supplementary conditions, and unique except for the possibility of differing internal symmetries. The price paid for this includes a Bleuler-Gupta-type indefinite metric and high dimensional state vectors, subject to gauge invariances for spin  $> \frac{1}{2}$ , in full analogy to spin 1 QED. The spin  $\frac{3}{2}$  state vectors representing a free massive particle consist of 12 component vectors (six representing positive energy states and six representing negative energy states): Choice of a particular gauge leaves only eight linearly independent solutions.

The Hayward theory starts from a Lagrangian density

$$\mathcal{L} = -\bar{\phi}(x)\partial_\mu\gamma_\mu\gamma_\nu\partial_\nu\phi(x) - M^2\phi(x)\phi(x), \quad (4)$$

minimization of the action integral of which leads to the equation of motion

$$(\partial_\mu\partial_\mu - M^2)\phi(x) = 0. \quad (5)$$

Here  $\phi(x)$  is the position space wave function; the  $\gamma_\mu$  form a four-vector of square matrices of dimension appropriate to the spin of the particle ( $12 \times 12$  for spin  $\frac{3}{2}$ ) which obey anticommutation relations of a Clifford algebra

$$[\gamma_\mu, \gamma_\nu]_+ = 2\delta_{\mu\nu}; \quad (6)$$

and the adjoint wave function is defined as

$$\bar{\phi} \equiv \phi^\dagger \gamma_4 \eta. \quad (7)$$

$\eta$  is +1 except for states which have  $M \neq 0$ , and which have timelike components nonvanishing in their rest frame. This is the indefinite metric, which allows a theory second order in time derivatives nonetheless to yield positive definite probability densities. Gauge invariant coupling of the  $\phi$  particles to a vector field  $A_\mu$  with coupling constant  $g$  is done via the minimal coupling substitution

$$\partial_\mu \rightarrow \partial_\mu - igA_\mu. \quad (8)$$

The Feynman propagator in this formalism is

$$D(x, x') = \frac{1}{2} \langle 0 | T[\phi(x)\phi(x')] | 0 \rangle, \quad (9)$$

where  $|0\rangle$  and  $\langle 0|$  are vacuum bra and ket states and  $T[ ]$  denotes the chronological product

$$\begin{aligned} T[\phi(x)\bar{\phi}(x')] &= \phi(x)\bar{\phi}(x') \text{ if } t \geq t' \\ &= (-)^{2s}\bar{\phi}(x')\phi(x) \text{ if } t' \geq t \end{aligned} \quad (10)$$

( $s$  denotes particle spin). This propagator is explicitly exhibited in the Hayward article for a particular gauge choice.

To use the Hayward formalism in the calculation of graphs where the delta exists in an intermediate state, having been created from, and decaying into, a nucleon, the vertex functions must be nonsquare matrices. The

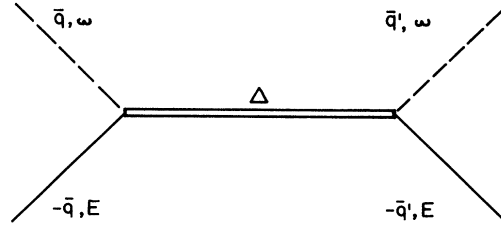


FIG. 1. Feynman diagram for pion-nucleon scattering with intermediate  $s$ -channel delta; momentum and energy variables as labeled.

delta excitation vertex is a four row by twelve column matrix, and the decay vertex is  $12 \times 4$ . Such vertex functions can be found in the work of Danos, Gillet, and Cauvin.<sup>6</sup> They construct vertices which exhibit the invariance properties of the appropriate interaction, which are Lorentz invariant, and which are the simplest possible combinations of the fields and their derivatives. Minimal coupling is invoked for electromagnetic vertices. Explicit forms for the vertex functions for both the Hayward and Rarita-Schwinger formalisms can be found in the Appendix.

In order to exhibit these vertices and the delta propagator in familiar notation and in a way easily compared with the Rarita-Schwinger results, I have chosen to consider three processes—pion nucleon scattering, photon nucleon scattering, and pion photoproduction—considering in each case only that graph which leads to the  $s$  channel excitation of a delta. Isospin indices will be suppressed. These processes will be presented as  $4 \times 4$  matrices which should be sandwiched between standard four-spinors  $(\bar{u}, u)$  in order to compute amplitudes. They will be exhibited using the Pauli  $2 \times 2$  spin matrices, so as to clearly represent the relative size of contributions in the low velocity limit. The vertex matrices presented represent the produce of three matrices,  $[4 \times 12] \cdot [12 \times 12] \cdot [12 \times 4] = [4 \times 4]$ . The particular representation of the Dirac  $\gamma$  matrices used separates the four-spinors into the upper two “large components” and the lower two “small components”:

$$u = [(E + m)/2m]^{1/2} \begin{pmatrix} \underline{1} \\ \bar{\sigma} \cdot \bar{p} \\ E + M \end{pmatrix} \chi, \quad (11)$$

where  $\underline{1}$  is the  $2 \times 2$  unit matrix,  $\bar{\sigma}$  are the three  $2 \times 2$  Pauli spin matrices,  $\chi$  is a Pauli two-spinor, and  $m$  is the nucleon mass.

### PION-NUCLEON SCATTERING

The pion-nucleon center-of-mass scattering amplitude, with momenta and energies defined in Fig. 1, is proportional to the following:

(a) The Rarita-Schwinger formalism (pseudoscalar pion)

$$-\frac{1}{3M} D\bar{u}_f \begin{pmatrix} (M + W) \left[ \bar{q}' \cdot \bar{q} - \frac{i}{2} \bar{\sigma} \cdot \bar{q}' \times \bar{q} \right] + \frac{M^2 - W^2}{M} \omega^2 & 0 \\ 0 & 0 \end{pmatrix} u_i. \quad (12)$$

(b) The Hayward formalism

$$-\frac{1}{2M}D\bar{u}_f \begin{pmatrix} (M+W) \left[ \bar{q}' \cdot \bar{q} - \frac{i}{2} \bar{\sigma} \cdot \bar{q}' \times \bar{q} \right] & 0 \\ 0 & (M-W) \left[ \bar{q}' \cdot \bar{q} - \frac{i}{2} \bar{\sigma} \cdot \bar{q}' \times \bar{q} \right] \end{pmatrix} u_i. \quad (13)$$

$W$  is the total center-of-mass energy,  $\omega$  is the pion total energy, and  $M$  is the delta mass. Each term in these  $2 \times 2$  arrays is itself a  $2 \times 2$  matrix.  $D$  represents the inverse of the quadratic energy denominator, which, in the case of a stable delta particle, would be

$$D = \frac{1}{(E + \omega)^2 - M^2 + i\epsilon}. \quad (14)$$

The appropriate form for this term accounting for the decay of the delta will be described later.

At the resonance peak ( $M = W$ ) these two formalisms give identical results. Moving off the peak by one half width in either direction, the RS amplitude picks up an extra term which is smaller than the dominant one by  $\Gamma/2M$  ( $\sim 0.05$ ). The additional term in the  $H$  amplitude is much smaller, being reduced from the dominant term by a factor  $(\Gamma/2M) q^2/(E+m)^2$  ( $\sim 0.007$ ). Despite the differences in angular dependence of the off-peak contributions, it will be difficult for experiments in the resonance region to give evidence favoring one formalism over the other.

### PHOTON-NUCLEON SCATTERING

The center-of-mass amplitude for elastic photon-nucleon scattering (see Fig. 2) is proportional to the following:

(a) The Rarita-Schwinger formalism

$$-\frac{1}{3M}D\bar{u}_f \begin{pmatrix} \left[ \bar{\epsilon}' \cdot \bar{\epsilon} - \frac{i}{2} \bar{\sigma} \cdot \bar{\epsilon}' \times \bar{\epsilon} \right] & 0 \\ 0 & 0 \end{pmatrix} + (M+W) \begin{pmatrix} \frac{1}{M+m} \left[ \left[ \frac{M+W}{M} k - \frac{\bar{k}' \cdot \bar{k}}{M+m} \right] (\bar{\epsilon}' \cdot \bar{\epsilon} + i \bar{\sigma} \cdot \bar{\epsilon}' \times \bar{\epsilon}) + \frac{1}{2(M+m)} (i \bar{\epsilon} \cdot \bar{k}' \times \bar{k} \bar{\sigma} \cdot \bar{\epsilon}' - \bar{\epsilon} \cdot \bar{k}' \bar{\epsilon}' \cdot \bar{k} - i \bar{\epsilon} \cdot \bar{k}' \bar{\sigma} \cdot \bar{\epsilon}' \times \bar{k}) \right] \\ -\frac{1}{(M+m)} \left[ -\bar{\epsilon}' \cdot \bar{k} \bar{\sigma} \cdot \bar{\epsilon} + \frac{i}{2} \bar{k} \cdot \bar{\epsilon}' \times \bar{\epsilon} - \frac{i}{2} \bar{\epsilon}' \cdot \bar{\epsilon} \bar{\sigma} \cdot \bar{k} \right] \end{pmatrix} \left. \begin{pmatrix} \frac{1}{M+m} \left[ -\bar{k}' \cdot \bar{\epsilon} \bar{\sigma} \cdot \bar{\epsilon}' + \frac{i}{2} \bar{k}' \cdot \bar{\epsilon} \times \bar{\epsilon}' - \frac{i}{2} \bar{\epsilon} \cdot \bar{\epsilon}' \bar{\sigma} \cdot \bar{k}' \right] \\ \bar{\epsilon}' \cdot \bar{\epsilon} - \frac{i}{2} \bar{\sigma} \cdot \bar{\epsilon}' \times \bar{\epsilon} \end{pmatrix} \right\} u_i. \quad (15)$$

Here  $\epsilon'_\mu = (0, \bar{\epsilon}')$  and  $\epsilon_\nu = (0, \bar{\epsilon})$  are the polarization four-vectors and  $m$  is the nucleon mass. Only the lowest nonvanishing orders in terms of  $k/M$  ( $\sim 0.2$  in the resonance region) are retained.

There are two separately gauge invariant  $\gamma N \Delta$  couplings appropriate for this formalism. The one exhibited here is the  $M1$  coupling, which experimentally has been shown to dominate in the resonance region. The other coupling, the electric quadrupole, is linear in the nucleon momenta as well as the photon momenta. Isospin dependence of the  $M1$  coupling prescribes equal amplitudes for  $\gamma p$  and  $\gamma n$  scattering.

(b) The Hayward formalism: The independent couplings for the  $\gamma N \Delta$  vertex appear in Ref. 6. The first and simplest, the current interaction, leads to the scattering amplitude

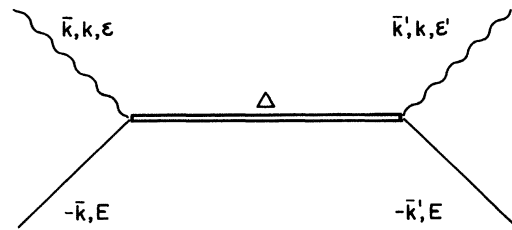


FIG. 2. Feynman diagram for photon-nucleon scattering with intermediate  $s$ -channel delta; momentum, energy, and polarization variables as labeled.

$$-\frac{1}{2M}D\bar{u}_f \begin{pmatrix} (M-W) \left[ \bar{\epsilon}' \cdot \bar{\epsilon} - \frac{i}{2} \bar{\sigma} \cdot \bar{\epsilon}' \times \bar{\epsilon} \right] & 0 \\ 0 & (M+W) \left[ \epsilon' \cdot \epsilon - \frac{i}{2} \bar{\sigma} \cdot \bar{\epsilon}' \times \bar{\epsilon} \right] \end{pmatrix} u_i. \quad (16)$$

The anomalous moment term of Ref. 6 must be included to produce favorable comparison with RS predictions (which have been shown to be in agreement with photoproduction data). Letting  $rM$  ( $r$  dimensionless) be the ratio of the coupling constant for the anomalous moment vertex to that of the current vertex, the lowest two nonvanishing orders of the added contributions are

$$\begin{aligned} & -\frac{1}{2M}D\bar{u}_f \left[ r \begin{pmatrix} -4\frac{k}{m}(M-W) \left[ \bar{\epsilon}' \cdot \bar{\epsilon} - \frac{i}{2} \bar{\sigma} \cdot \bar{\epsilon}' \times \bar{\epsilon} \right] & 3\frac{(M+W)}{M}(\bar{\epsilon}' \cdot \bar{\epsilon} \bar{\sigma} \cdot \bar{k}' - \bar{\epsilon} \cdot \bar{k}' \bar{\sigma} \cdot \bar{\epsilon}') \\ \frac{(M+W)}{M}(\bar{\epsilon}' \cdot \bar{\epsilon} \bar{\sigma} \cdot \bar{k} - \bar{\epsilon}' \cdot \bar{k} \bar{\sigma} \cdot \bar{\epsilon}) & 0 \end{pmatrix} \right. \\ & \left. + r^2 \begin{pmatrix} 4\frac{(M+W)}{M^2} \left[ -\bar{\epsilon}' \cdot \bar{\epsilon} \bar{k}' \cdot \bar{k} + \bar{\epsilon}' \cdot \bar{k} \bar{\epsilon} \cdot \bar{k}' - \frac{i}{2} \bar{\epsilon}' \cdot \bar{k}' \times \bar{k} \bar{\sigma} \cdot \bar{\epsilon} + \frac{i}{2} \bar{k}' \cdot \bar{\epsilon} \times \bar{\epsilon}' \bar{\sigma} \cdot \bar{k} \right] & 0 \\ 0 & 0 \end{pmatrix} \right] u_i. \quad (17) \end{aligned}$$

Isospin dependence of these amplitudes is not specified by the theory<sup>7</sup> and, in lieu of a dynamic theory of the structure of baryons, should be adjusted to fit the data.

The leading term in the RS formalism is identical to the leading term of the current vertex contribution in the Hayward formalism [Eq. (17)]. The energy dependence of these two terms causes them to vanish at resonance, how-

ever. Similarities exist between the remaining terms in the RS amplitude and the anomalous moment terms of Eq. (18), but no one-to-one matching is possible.

Appropriate choice of the anomalous transition moment (equivalently  $r$ ) can be made to produce similar results: An example of such a choice will be illustrated later in this paper.

### PHOTOPRODUCTION OF PIONS

In the center of mass system, the pion photoproduction amplitude (shown in Fig. 3), is proportional to the following:

(a) The Rarita-Schwinger formalism (pseudoscalar pion)

$$-\frac{1}{3M}D\bar{u}_f \begin{pmatrix} \frac{M+W}{M} \left[ -\frac{\omega}{2}(M-W) + \frac{M}{(M+m)} \bar{q}' \cdot \bar{k} - \frac{(M-W)k\omega}{(M+m)} \right] \bar{\sigma} \cdot \bar{\epsilon} & (M+W) \left[ \bar{q}' \cdot \bar{\epsilon} - \frac{i}{2} \bar{\sigma} \cdot \bar{q}' \times \bar{\epsilon} \right] \\ + \frac{M}{(M+m)} (\bar{\epsilon} \cdot \bar{q}' \bar{\sigma} \cdot \bar{k} - i \bar{\epsilon} \cdot \bar{q}' \times \bar{k}) & \\ (M-W) \left[ \bar{q}' \cdot \bar{\epsilon} - \frac{i}{2} \bar{\sigma} \cdot \bar{q}' \times \bar{\epsilon} \right] & 0 \end{pmatrix} u_i. \quad (18)$$

Terms of order  $k^2/M^2$  and higher, relative to the leading terms, have been discarded.

(b) The Hayward formalism

$$-\frac{1}{2M}D\bar{u}_f \begin{pmatrix} r \frac{(M+W)}{M} (\bar{q}' \cdot \bar{\epsilon} \bar{\sigma} \cdot \bar{k} - \bar{q}' \cdot \bar{k} \bar{\sigma} \cdot \bar{\epsilon}) & (M-W) \left[ 1 + r \frac{k}{m} \right] \left[ \bar{q}' \cdot \bar{\epsilon} - \frac{i}{2} \bar{\sigma} \cdot \bar{q}' \times \bar{\epsilon} \right] \\ (M-W) \left[ \bar{q}' \cdot \bar{\epsilon} - \frac{i}{2} \bar{\sigma} \cdot \bar{q}' \times \bar{\epsilon} \right] & 0 \end{pmatrix} u_i. \quad (19)$$

Higher order terms, as in (a) above, have been discarded. Isospin dependence yields coefficients of 1,  $-1$ , 2, and 2 for the processes  $\gamma n \rightarrow p\pi^-$ ,  $\gamma p \rightarrow n\pi^+$ ,  $\gamma p \rightarrow p\pi^0$ , and  $\gamma n \rightarrow n\pi^0$ , respectively, for the RS amplitude. The Hayward case prescribes the standard isospin vector coupling

coefficients for the  $\pi n$  final state, but the relation between the  $\gamma p$  and  $\gamma n$  amplitudes is not specified.

At resonance ( $M=W$ ) the forms of these two amplitudes become very similar, suggesting that an appropriate choice of  $r$  might produce good agreement (which shall be

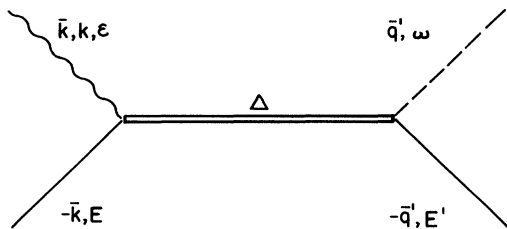


FIG. 3. Feynman diagram for pion photoproduction from a nucleon, with intermediate  $s$ -channel delta; momentum, energy, and polarization variables as labeled.

demonstrated). Quite dissimilar terms become noticeable when the energy is merely one half width from the resonance peak, and discrepancies in prediction should be measurable in integrated cross sections, and even more so in particular spin and angular differential cross sections.

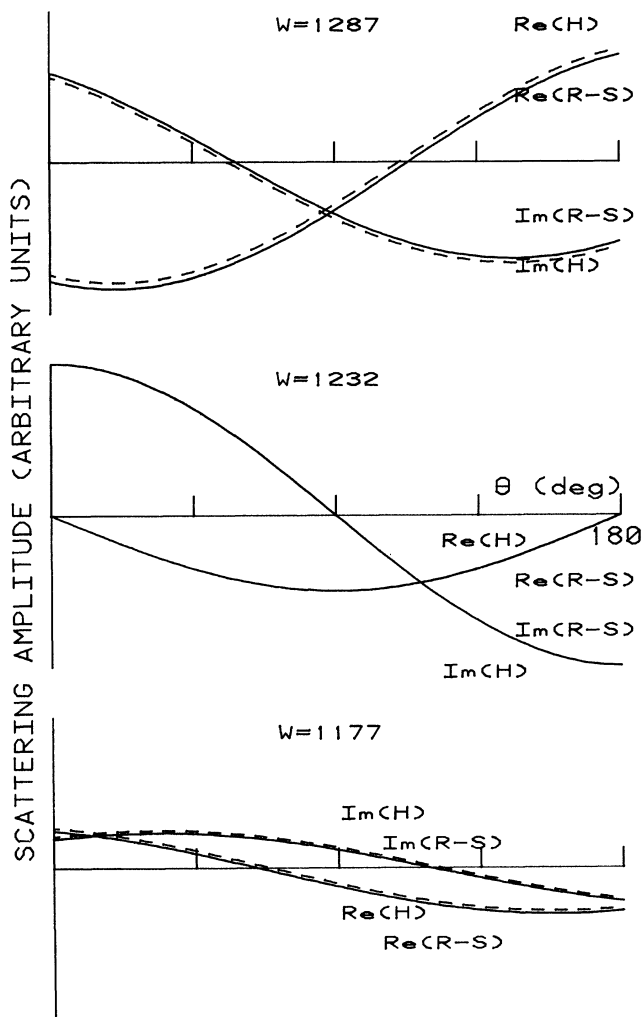


FIG. 4. Angular dependence of pion scattering amplitudes at three energies in the resonance region (solid line—RS amplitude; dashed line—Hayward amplitude).

## NUMERICAL ILLUSTRATION

In an attempt to somewhat quantify comparison of the three Rarita-Schwinger and Hayward amplitudes, Figs. 4–6 present fixed total energy angular dependences of these amplitudes. They are shown on arbitrary scales, fixed such that the imaginary parts of the RS and Hayward amplitudes are equal in the forward direction at  $W=1232$  MeV (at resonance). Angular dependences are shown at the peak, and at a total energy one half-width on either side. For the purpose of these graphs, the energy denominator was chosen to be

$$D = \frac{1}{W^2 - M^2 + iM\Gamma} \quad (20)$$

with  $\Gamma=110$  MeV. The illustrated values correspond to the situation in which all polarization (nucleon and photon, initial and final) are perpendicular to the scattering plane. The amplitudes and angles are expressed in the center of mass frame.

Figure 4 serves to illustrate the fact that with appropri-

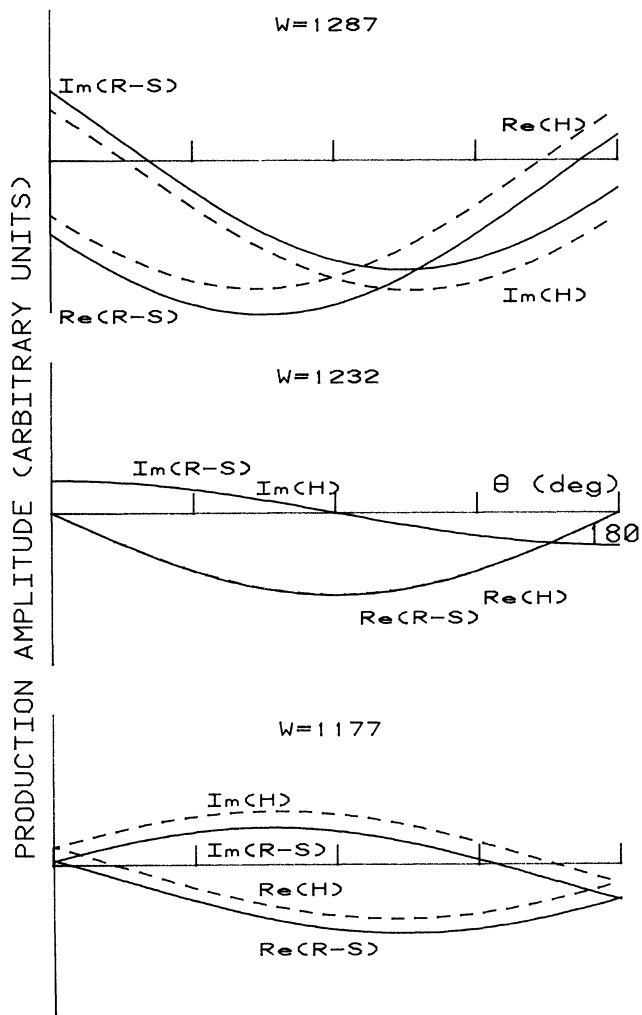


FIG. 5. Angular dependence of photon scattering amplitude at three energies in the resonance region (solid line—RS amplitude; dashed line—Hayward amplitude).

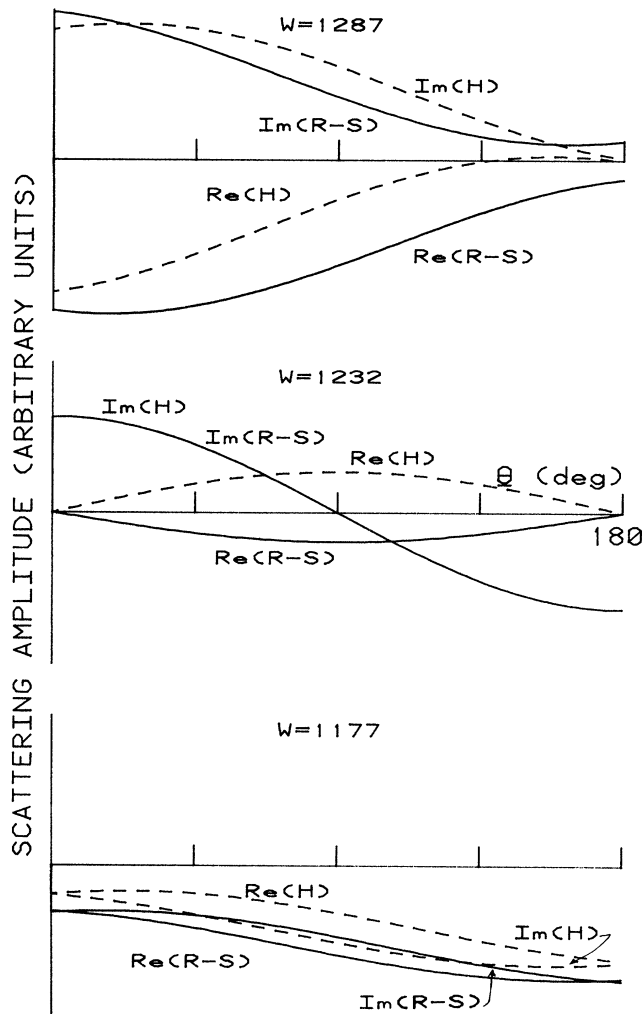


FIG. 6. Angular dependence of pion photoproduction amplitude at three energies in the resonance region (solid line—RS amplitude; dashed line—Hayward amplitude).

ate choice of coupling constants, the two formalisms give effectively identical predictions of  $\pi$ -N scattering amplitudes. Whereas the discrepancy between the two becomes greater proportional to the distance from the resonance peak, terms in the total  $\pi$ N amplitude other than the 3-3 resonance term should obscure the difference.

Figure 5 shows a comparison of the two formalisms for pion photoproduction. In the  $W = 1232$  MeV calculation the value of  $r$ , representing the size of the anomalous transition moment, and the size of the  $\gamma$ N $\Delta$  vertex coupling constant, were chosen to give the best agreement between the two. Nearly perfect agreement at this energy leads to quite noticeable differences of prediction at energies one half-width away. Specific energies, scattering angles, and/or polarization directions could be selected which would emphasize these differences, and allow experimental results to choose the amplitude in best agreement. (Since for spin  $\frac{1}{2}$ , the Hayward theory coincides with standard Dirac theory,  $s$  and  $u$  channel processes with nucleon intermediate states will be treated identically

in the two formalisms.) The value of  $r$  chosen using photoproduction calculations is used for the calculation of photon scattering.

Figure 6 shows angular distribution for elastic photon scattering calculated using the two formalisms. The value of the Hayward  $N\gamma\Delta$  current coupling constant is chosen so that the imaginary part of the  $W = 1232$  MeV curve will match the result from RS, while the ratio of the anomalous moment coupling constant to that for the current vertex is the same as was used in the photoproduction fit. Whereas the predictions of the two formalisms are in qualitative agreement at  $W = 1287$  and  $1177$  MeV, at resonance, the real parts have opposite sign. Other choices of this ratio can improve this particular discrepancy, but at the expense of the fit at other energies. Using coupling constants deduced from the photoproduction fit can give a parameter-free prediction of the curves of Fig. 6. This would cause an enhancement of the Hayward predictions (dashed lines) by a factor of 6.7, and put the two formalisms in complete disagreement.

No attempt has been made to find the optional set of Hayward coupling constants which would give the best agreement with RS predictions. The above calculations are to illustrate the fact that simultaneous comparison of predictions with data using the two approaches for the three processes considered should clearly rule in favor of one approach over the other. They *cannot* agree with each other within the resonance region—experiment must support one, or neither.

Two aspects of the data of Figs. 4–6 warrant further comment. Whereas at resonance, one expects the real part of the scattering amplitude to vanish, each figure shows real parts of significant size at  $W = 1232$  MeV. This is because a relativistic propagator includes both a particle moving forward in time, and an antiparticle moving backward in time. In the center of mass system the first possibility corresponds to a pure (resonant) spin  $= \frac{3}{2}$  amplitude, but the second contains all multipoles and is not totally imaginary at resonance. In  $\gamma$ N scattering, the terms corresponding to a propagating antiparticle are of the same order of magnitude as the particle propagation contributions. The other matter refers specifically to the  $W = 1177$  graph in Fig. 6. For both formalisms the imaginary part of the forward scattering amplitude is negative—a violation of unitarity. This would not be a problem in a complete calculation, where the unitarity of the  $S$  matrix is guaranteed by the presence of additional contributions which provide a slowly varying background to the  $\Delta$  exchange term in the resonance region.

#### ENERGY DENOMINATOR

The form of the propagator, particularly the energy dependence of the form factor (if any) and the denominator, depends upon the underlying theoretical assumptions.

If the delta is treated as a fundamental field in a Lagrangian field theory, it is assumed to be a stable particle—the mass is represented by a point on the real axis of the complex energy plane. With fundamental nucleon and pion fields, the presence of a  $N\pi$  state with the same quantum numbers as the delta but at lower energy

will “dress” the bare delta, giving the physical delta a shifted mass and a nonzero width.

Theories exemplified by the Chew-Low model do not introduce the delta in the Lagrangian but find that the various manifestations of the delta “resonance” can be explained by sums of states  $N\pi$ ,  $N\pi\pi$ ,  $N\pi\pi\pi$ , . . . . Such approaches often use a resonance denominator as a convenient parametrization of behavior in the resonance region, but would not expect the spin dependence to be so rigidly described as by the RS or Hayward propagators. From this point of view the introduction of a separate delta field brings the danger of double counting, yet there are ways to avoid or at least minimize these problems while treating the delta as a fundamental field.<sup>8</sup>

$S$  matrix theory allows, in addition to poles on the real axis in the complex energy plane, fixed off-axis poles on the second sheet, i.e., resonances with mass  $M$  and width  $\Gamma$  which do not vary with energy,

$$D = \frac{1}{s - M^2 + iM\Gamma}, \quad (21)$$

where  $s$  is the square of the total center of mass energy. Crossing symmetry implies an image pole, off axis, at  $u = M^2 - iM\Gamma$  ( $u$  is the Mandelstam crossed energy variable).

When processes are treated in a truncated Hilbert space (considering nucleons and deltas as the only baryons, for example), often fundamental requirements of amplitudes like unitarity and crossing symmetry are lost. Contributions to the amplitude which are unitary separately are not easily combined into a unitary sum. Such difficulties can produce obvious errors. In Compton scattering, the amplitude should be real below the  $N\pi$  threshold. A fixed pole delta violates this requirement, even when crossing symmetry is accounted for. In the  $S$  matrix approach, the imaginary parts of the sum of the  $s$  and  $u$  channel delta amplitudes are cancelled exactly, below  $N\pi$  threshold, by the summed contributions of  $s$  and  $u$  channel graphs of all higher resonances. This must be accounted for in a realistic calculation. A further requirement of Compton scattering is that the threshold cross section must equal the Thompson cross section, and this is accomplished by treating only the  $s$  and  $u$  channel nucleon poles. Delta  $s$  and  $u$  exchange contributions do not vanish at threshold, and again must be cancelled by the effects of processes not explicitly included. Olsson<sup>9</sup> has shown that the effects of unitarizing amplitudes consisting of a single resonant pole and nonresonant background can be treated by the introduction of energy dependent widths and vertex functions into the propagators. The precise form of the width function as well as a multiplicative energy dependent factor for the propagator depend upon what terms are included in the treatment (no background, background, other resonances?) as well as upon which process is being considered. An example of Olsson's results, in the case where  $s$  channel delta exchange is added to a nonresonant background for the treatment of  $N\pi$  scattering is

$$D = \frac{V}{s - M^2 + iM\Gamma}, \quad (22)$$

where

$$\Gamma = 0.31 \frac{(E+m)(\sqrt{s}+M)}{6s} q^3, \quad (23)$$

and the vertex factor  $V$  is proportional to

$$\frac{(E+m)(\sqrt{s}+M)}{s} q^2. \quad (24)$$

In the case of  $\gamma N$  scattering,  $V$  is proportional to  $k^2$ , the square of the photon momentum. The  $q$  dependence of the width guarantees zero width at (and below) pion threshold, and the  $k^2$  vertex function for  $\gamma N$  scattering ensures a zero contribution at photon threshold.

Exhibited in Fig. 7 is the energy dependence of the  $\pi N$  scattering phase shift in the neighborhood of the delta peak, in the spin =  $\frac{3}{2}$ , isospin =  $\frac{3}{2}$  channel. The solid line represents a fit to the experimental phase shifts,<sup>10</sup> the dashed line represents the phase shifts of a fixed pole of width 110 MeV, and the dot-dashed line represents the parametrization of Olsson. The discrepancy between experiment and Olsson's result can be nearly eliminated with the inclusion of appropriate background terms.

A treatment of the resonating ratio  $D$ , following Olsson, with  $V$  and  $\Gamma$  chosen appropriate to the process under consideration and to the number of and kind of amplitudes included, should produce reasonable cross section predictions in the resonance region.

Crossing symmetry implies the need to treat the  $u$  channel delta exchanges in combination with the  $s$  channel exchanges discussed herein. Even in the center of mass system, the Rarita-Schwinger and Hayward propagators for this case become extremely tedious and complicated. For treatment of processes from threshold through the delta resonance region, the  $u$  delta contributions can be implicitly included via the energy dependent width and vertex function of the  $s$  channel propagator. For pion scattering and photoproduction, the  $u$  channel delta pole is always more distant (in the energy plane) than the  $N^*(1470)$ , the next higher nucleon resonance which is seldom explicitly included. In Compton scattering at threshold, the  $s$  and  $u$  channel delta poles are equidistant, but

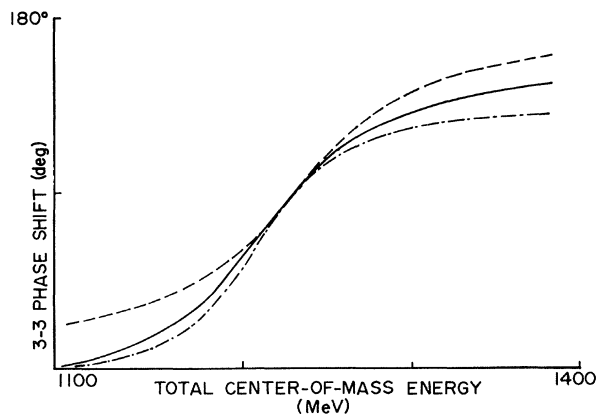


FIG. 7. Scattering phase shift for pion-nucleon scattering in total spin =  $\frac{3}{2}$ , total isospin =  $\frac{3}{2}$  channel: solid line—fit to data; dashed line—fixed delta pole; dot-dashed line—parametrization of Olsson.

their sum must be canceled here by other processes (simulated by  $k^2$  in the vertex function), and thus even here the  $u$  delta exchange can be consistently omitted.

#### ACKNOWLEDGMENTS

The author would like to thank M. Danos for several helpful discussions on the topics of this paper. This research was supported by a grant from the Research Corporation.

#### APPENDIX

The amplitudes calculated in this paper are related to two three-particle vertices, the  $N\pi\Delta$  and the  $N\gamma\Delta$ . The form of these is shown below:

(a) The Rarita-Schwinger formalism:

$N\pi\Delta$  vertex:

$$g_\pi q_\mu ,$$

$N\gamma\Delta$  vertex:

$$-g_\gamma \left[ \epsilon_\mu - \frac{\gamma_\nu \epsilon_\nu k_\mu}{(M+m)} \right] \gamma_5 ,$$

where  $g_\pi$  and  $g_\gamma$  are the coupling constants for the vertices, and the  $\mu$  index (0,1,2,3) is to be contracted with the four-vector index on the RS  $\frac{3}{2}$  spinor in the final state. Repeated indices are summed. A form for the RS propagator is given in Eq. (3).

(b) The Hayward formalism:

$N\pi\Delta$  vertex:

$$G_\pi \gamma_5 q_\mu D_\mu^\dagger ,$$

$N\gamma\Delta$  current vertex:

$$-iG_{\gamma c} \epsilon_\mu D_\mu^\dagger ,$$

$N\gamma\Delta$  anomalous moment vertex:

$$-iG_{\gamma am} (\gamma_\mu D_\nu^\dagger - \gamma_\nu D_\mu^\dagger) (k_\mu \epsilon_\nu - k_\nu \epsilon_\mu) ,$$

where  $G_\pi$ ,  $G_{\gamma c}$ , and  $G_{\gamma am}$  are the coupling constants.  $D_\mu^\dagger$  is a  $4 \times 12$  matrix of the form ( $k = 1, 2, 3$ ),

$$D_0^\dagger = \frac{9}{8} \begin{bmatrix} 0 & 0 & 0 & I \\ 0 & -I & 0 & 0 \end{bmatrix}, \quad D_k^\dagger = \begin{bmatrix} 0 & G_k^\dagger & -F_k^\dagger \\ F_k^\dagger & 0 & 0 & -F_k^\dagger \end{bmatrix},$$

where  $I$  is the  $2 \times 2$  unit matrix; then  $G_k^\dagger$  are  $2 \times 2$  matrices with elements

$$\begin{aligned} (G_1^\dagger)_{m,m'} &= 2\sqrt{3}(C_{m'1m}^{1/211/2} - C_{m-1m'}^{1/211/2}), \\ (G_2^\dagger)_{m,m'} &= -i2\sqrt{3}(C_{m'1m}^{1/211/2} + C_{m-1m'}^{1/211/2}), \\ (G_3^\dagger)_{m,m'} &= -2\sqrt{6}C_{m'0m}^{1/211/2}; \end{aligned}$$

and  $F_k^\dagger$  are  $2 \times 4$  matrices with elements

$$\begin{aligned} (F_1^\dagger)_{m,m'} &= \sqrt{3/2}(C_{m'1m}^{1/213/2} - C_{m'-1m}^{1/213/2}), \\ (F_2^\dagger)_{m,m'} &= i\sqrt{3/2}(C_{m'1m}^{1/213/2} + C_{m'-1m}^{1/213/2}), \\ (F_3^\dagger)_{m,m'} &= -\sqrt{3/2}C_{m'0m}^{1/213/2}. \end{aligned}$$

The  $C$ 's are Clebsch-Gordan coefficients. The rows and columns of the  $G$  matrices are labeled  $m = +\frac{1}{2}, -\frac{1}{2}$ ; for the  $F$  matrices,  $m' = \frac{3}{2}, +\frac{1}{2}, -\frac{1}{2}, -\frac{3}{2}$ .

The Hayward propagator, in the simplest case of a  $\Delta$  particle in its center of mass frame and in a gauge (analogous to the Lorentz gauge in QED) where gauge-dependent terms (analogous to longitudinal photons) vanish, is a  $12 \times 12$  diagonal matrix. The top four diagonal elements have the value  $(M+W)/2M$ ; diagonal elements 6–10 have the value  $(M-W)/2M$ ; all other matrix elements vanish.

<sup>1</sup>W. Rarita and J. Schwinger, Phys. Rev. **60**, 61 (1941).

<sup>2</sup>S. Gasiorowicz, *Elementary Particle Physics* (Wiley, New York, 1966).

<sup>3</sup>J. D. Bjorken and S. D. Drell, *Relativistic Quantum Mechanics* (McGraw-Hill, New York, 1964).

<sup>4</sup>G. Velo and D. Zwanziger, Phys. Rev. **186**, 1337 (1969).

<sup>5</sup>R. W. Hayward, The Dynamics of Fields of Higher Spin, National Bureau of Standards Monograph No. 154, 1976.

<sup>6</sup>M. Danos, V. Gillet, and M. Cauvin, *Methods in Relativistic Nuclear Physics* (North-Holland, Amsterdam, 1983).

<sup>7</sup>M. Danos, private communication.

<sup>8</sup>A. S. Rinat, Phys. Rev. C **27**, 2425 (1983); K. Holinde, *ibid.* **27**, 2428 (1983).

<sup>9</sup>M. G. Olsson, Nucl. Phys. **B78**, 55 (1974).

<sup>10</sup>J. R. Carter, D. V. Bugg, and A. A. Carter, Nucl. Phys. **B58**, 378 (1972).